Journal of Pharmacological Sciences 148 (2022) 65–72

Contents lists available at ScienceDirect

Journal of Pharmacological Sciences

journal homepage: www.elsevier.com/locate/jphs

Full Paper

Nafamostat protects against early brain injury after subarachnoid hemorrhage in mice

Hirofumi Matsubara [a, b], Takahiko Imai [a], Shohei Tsuji [a], Natsumi Oka [a], Yusuke Egashira [a, b], Yukiko Enomoto [a], Noriyuki Nakayama [a], Shinsuke Nakamura [a], Masamitsu Shimazawa [a], Toru Iwama [b], Hideaki Hara [a, *]

[a] Molecular Pharmacology, Department of Biofunctional Evaluation, Gifu Pharmaceutical University, Gifu, Japan
[b] Department of Neurosurgery, Gifu University Graduate School of Medicine, Gifu, Japan

ARTICLE INFO

Article history:
Received 29 July 2021
Received in revised form
1 October 2021
Accepted 19 October 2021
Available online 23 October 2021

Keywords:
Nafamostat
Subarachnoid hemorrhage
Early brain injury
Thrombin

ABSTRACT

This study aimed to evaluate the effects of nafamostat, a serin protease inhibitor, in the management of subarachnoid hemorrhage (SAH). SAH was induced by endovascular perforation in male mice. Nafamostat was administered intraperitoneally four times immediately after SAH induction. Cerebral blood flow, neurological behavior tests, SAH grade and protein expression were evaluated at 24 h after SAH induction. In the *in vitro* model, human brain microvascular endothelial cells (HBMVECs), HBVECs were exposed to thrombin and hypoxia for 24 h; nafamostat was administered and the protein expression was evaluated.

Eighty-eight mice were included in *the in vivo* study. Fifteen mice (17%) were excluded because of death or procedure failure. Nafamostat exerted no significant effect on the SAH grade or cerebral blood flow; however, it improved the neurological behavior and suppressed the thrombin and MMP-9 expression. In addition, nafamostat suppressed the ICAM-1 expression and p38 phosphorylation in *the in vitro* study.

Nafamostat has a protective effect against HBMVEC after exposure to thrombin and hypoxia, suggesting its role in improving the neurological outcomes after SAH. These findings indicate that nafamostat has the potential to be a novel therapeutic drug in the management of SAH.

1. Introduction

Subarachnoid hemorrhage (SAH) is a severe cerebrovascular disease that mainly occurs due to aneurysm rupture.[1,2] Advancements have been made in the intervention (clipping or coiling) and postoperative care management of SAH; however, mortality and poor outcomes remain high.[3] SAH-induced brain damage can be classified as early brain injury and delayed cerebral ischemia.[1] Early brain injury involves neuroinflammation, blood–brain barrier (BBB) disruption, platelet aggregation, and endothelial injury, which are aggravating factors in delayed cerebral ischemia or outcomes.[1,4] Therefore, effective therapeutic or pharmaceutical management is necessary to improve SAH-induced early brain injury.

Currently, coronavirus disease (COVID-19) is rapidly spreading worldwide.[5] Vaccination for COVID-19 has been used; despite this, cases and mortality rate continue to increase. Therefore, the development of drugs for the management of COVID-19 remains a significant and urgent issue that requires worldwide attention. Among the proposed drugs, nafamostat has recently become a drug of interest for the treatment of COVID-19[6,7].

Nafamostat is a serine protease inhibitor that has been used for the management of pancreatitis, disseminated intravascular coagulation, and hemodialysis. Nafamostat has anti-inflammatory and endothelial protective effects; furthermore, studies have shown this protective effect in experimental models of cerebral ischemic stroke.[8–10] Additionally, it has been reported the efficacy of nafamostat for vasospasm after SAH[11,12]; however, its effect on early brain injury remains unclear.

* Corresponding author. Molecular Pharmacology, Department of Biofunctional Evaluation, Gifu Pharmaceutical University, 1-25-4, Daigaku-nishi, Gifu, Japan.. Tel.: +81 58 230-8126
E-mail address: hidehara@gifu-pu.ac.jp (H. Hara).
Peer review under responsibility of Japanese Pharmacological Society.

https://doi.org/10.1016/j.jphs.2021.10.007

Experimental models have shown the relationship of thrombin, a serin protease coagulation protein, in the development of BBB disruption or brain edema after intracerebral hemorrhage, cerebral ischemia and SAH.[13–16] Argatroban, a thrombin inhibitor, has been shown to have protective effect against early brain injury after SAH[16]; similarly, nafamostat exerts it pharmaceutical effect as also has the thrombin inhibitor. Therefore, we investigated the protective effects of nafamostat against early brain injury through *in vivo* (endovascular perforation SAH murine model) and *in vitro* (human brain microvascular endothelial cells [HBMVECs]) studies.

2. Material & methods

All animal protocols were approved by and were conducted in accordance with the guidelines of the experimental committee of Gifu Pharmaceutical University, Japan.

2.1. Animal preparation

A total of 114 male ddY mice (aged, 8 weeks old; body weight, 33–40 g) purchased from Japan SLC, Inc. (Hamamatsu, Shizuoka, Japan) were used in the following three experiments. We carefully considered minimized the suffering and the number of animals used. All animals were housed in a controlled environment (24 ± 2 °C; 12 h/12 h light/dark cycles). They received standard laboratory food and filtered clean water ad libitum.

2.2. SAH induction and CBF study

An SAH was induced through the endovascular perforation technique, as previously described.[17] In brief, general anesthesia containing a mixture of 70% NO_2, 20% oxygen, and 2.0–3.0% isoflurane was administered using an animal general anesthesia machine (Soft Lander; Sin-ei Industry Co., Ltd., Saitama, Japan). After skin incision, SAH was induced by inserting a 5–0 nylon monofilament from the right external carotid artery (ECA) to the internal carotid artery (ICA) bifurcation. After the perforation, the filament was removed, and the ECA coagulated. This procedure was performed after the common carotid artery was temporary occluded. After the operation, the mice were maintained under similar conditions as the preoperative environment. The skin was incised in the sham group.

Cerebral blood flow (CBF) was measured in three different periods (pre-procedure, post-procedure, and 1 d post-procedure) using LSFI (LSFG-ANM; Soft-care Co., Ltd.; Fukuoka, Japan). CBF measurements were performed under general anesthesia.

2.3. Nafamostat administration

The mice were randomly assigned to four groups; sham, vehicle and two nafamostat (0.1, and 1 mg/kg) groups. The experimental procedure is illustrated in Fig. 1A. In the nafamostat groups, nafamostat was (N0959, Tokyo Chemical Industry Co., Ltd., Tokyo, Japan) diluted in 5% glucose and administered intraperitoneally (i.p.) at 0, 2, 4, and 6 h post-procedure. In the vehicle groups, 5% glucose was administered in the same manner. In the sham group, no solvent was administered.

2.4. Neurological behavior test

Neurological assessment was performed in a quiet and dimly lit room. The modified neurological score (mNS) was used to evaluate the differences in the neurological behavior between the groups.[18] In this study, the mNS was based on a 24-point scoring system. The scores were determined based on the following eight tests: spontaneous activity, climbing, balance, side stroking, vibrissae touch (i.e., stroke of whiskers), visual (i.e., tip toward each eye), forelimb use, and hindlimb use. Each mouse was able to obtain three possible points in each test based on the neurological presentation. Lower scores indicated more severe neurological deficits.

2.5. SAH grading score

The mice's brains were removed and examined after the neurological behavior test. The SAH grading score was used to assess subarachnoid clot volume.[19] This scale divides the basal brain into five segments. Each segment is assigned a grade from 0 to 3, based on the amount of SAH, as follows: 0 indicates no SAH; 1, minimal SAH; 2, moderate SAH with recognizable arteries; and 3, SAH obliterated the cerebral arteries. The animals received a total score ranging from 0 to 15 after adding the scores from the five segments.

2.6. Hb assay

Twenty-four hours SAH, mice were intraperitoneally administered with pentobarbital sodium and transcardially perfused with saline. The brains were removed quickly, and the SAH volume was quantified using a spectrophotometric assay of the hemoglobin content in the whole brain. After brain perfusion, the brain sample was homogenized and centrifuged for 30 min at 13,000×*g* at room temperature (25 °C). Then, 200 μL of the reagent (QuantiChrom Hemoglobin Assay Kit; BioAssay Systems, Hayward, CA, USA) was added to a 50 μL aliquot of the supernatant. After 5 min, the optical density was read at 400 nm using a spectrophotometer (Skan It RE for Varioskan 133 Flash 2.4; Thermo Fisher Scientific, Waltham, MA, USA). The total hemoglobin content was expressed in microliters (μL).[20]

2.7. Coagulation time

One hour after the administration of nafamostat or 5% glucose, mice were injected intraperitoneally with pentobarbital sodium. Blood was collected from the inferior vena cava using 3.2% sodium citrate (sodium citrate: blood = 1: 9). Blood samples were centrifuged for 15 min at 1500×*g* and at 4 °C after the collection as soon as possible. The plasma was collected, and the coagulation time was measured with a Thrombo-check kit PT or APTT (12,500, 12,980, Sysmex Co., Ltd.; Kobe, Japan).

2.8. Cell culture and combined thrombin and hypoxia stress

Human primary brain microvascular endothelial Cells (HBMVECs) (ACBRI 376, Cell Systems Inc., Cambridge, Massachusetts, USA) were cultured dishes in CS-C Complete Medium Kit R (4Z0500R, Cell Systems Inc.), medium containing 10% fetal bovine serum (FBS), and CultureBoost-R™ (containing human recombinant growth factors). The cells were incubated at 37 °C in a humidified 5% CO_2 atmosphere until they reached confluence. Cells were seeded on a plate which was coated with collagen (Cellmatrix®; Nitta Zelatin Inc., Osaka, Japan). The medium was changed every two days.

To evaluate the effect of nafamostat on SAH in endothelial cells, a combined thrombin and hypoxia stress model was utilized in HBMVECs. HBMVECs were seeded at 30,000 cells/well in 24 well plates and cultured for 3 d. The cells were incubated in a Medium Without Serum Kit (4Z3500R, Cell Systems Inc.), medium containing CultureBoost-R™ (containing human recombinant growth factors), and serum-free medium in an oxygen-free incubator (94% N2, 5% CO2, and 1% O2) for 24 h. Human thrombin (T6884,

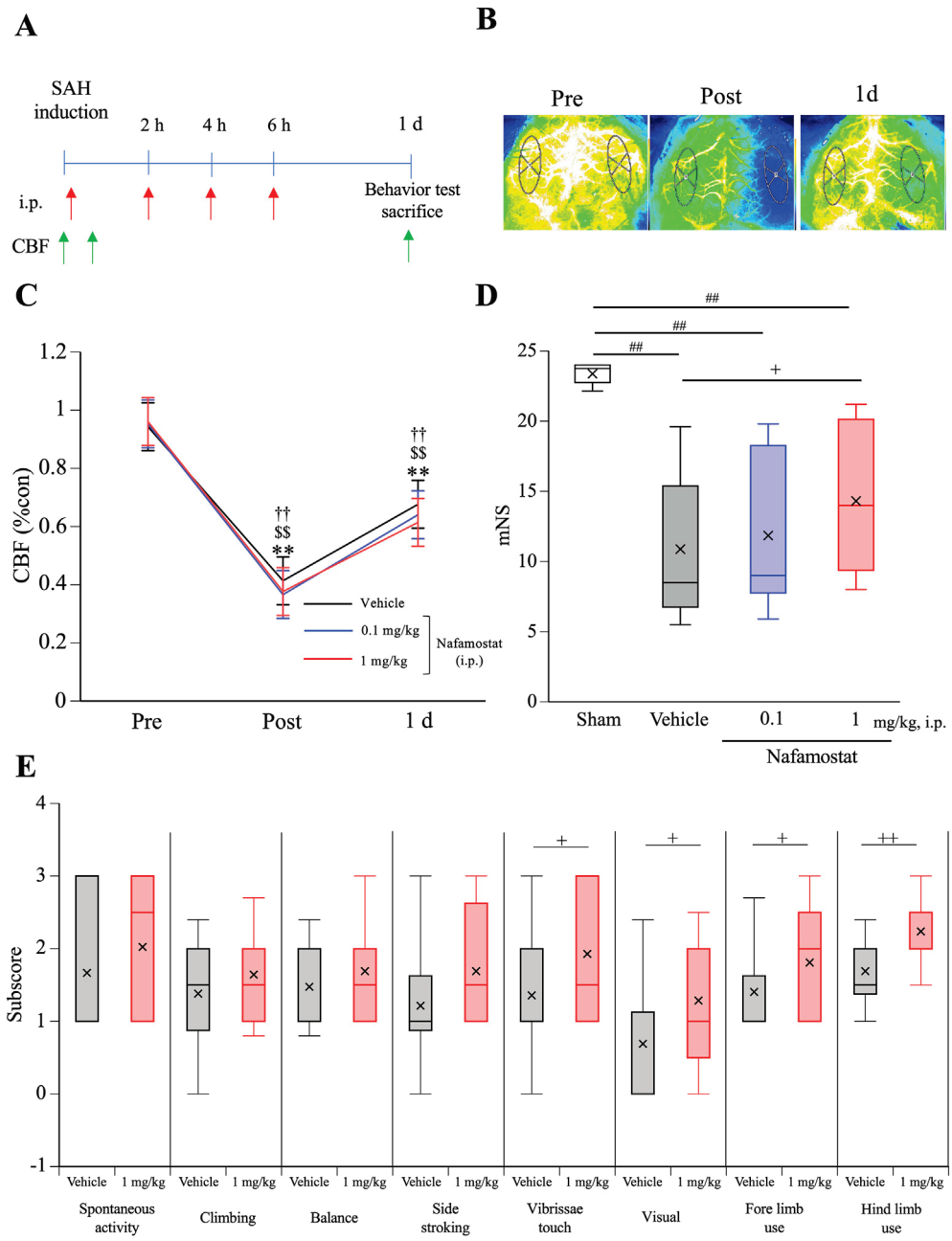

Fig. 1. (A) The protocol for evaluating the effect of nafamostat to subarachnoid hemorrhage (SAH). Nafamostat or 5% glucose were administrated four times. A behavior test (modified neurological score: mNS) was evaluated 24 h after the SAH. Cerebral blood flow (CBF) was measured three times by using Laser speckle flow imaging (LSFI). (B) A representative case of LSFI after SAH induction. (C) The CBF findings (%) of the contralateral side. The CBF immediately and 1 d post-procedure were significantly lower compared to pre-procedure; however, no significant differences was observed between groups. (D) Total score of mNS. mNS was significantly worse after SAH induction. However, administration of 1 mg/kg nafamostat significantly improved the mNS. (E) Subscores of mNS on vehicle and nafamostat 1 mg/kg groups. Sham, n = 8; Vehicle, n = 21; Nafamostat 0.1 mg/kg, n = 13; Nafamostat 1 mg/kg, n = 21. $^{\dagger\dagger}p < 0.01$, vs. pre-procedure on vehicle, $^{\$\$}$ $p < 0.01$, vs. pre-procedure on 0.1 mg/kg, $^{**}p < 0.01$, vs. pre-procedure on 1 mg/kg, Dunnet's test. $^{\#\#}p < 0.01$, vs. sham, Wilcoxon test.$^{+}p < 0.05$, $^{++}$ $p < 0.01$, vehicle vs. 1 mg/kg, Wilcoxon test.

Sigma–Aldrich Co., Ltd.; St. Louis, Missouri, USA) was diluted with sterilized water to achieve a final concentration of 5 U/ml. Different doses of nafamostat (0.1, 1.0, and 10 μmol/L) were added to the medium immediately before the administration of combined thrombin and hypoxic stress. The concentrations of nafamostat were based on the previous reports.[21] Control cells were incubated in complete medium. Western blot assays were performed 24 h after the combined thrombin and hypoxic stress.

2.9. Western blotting

The brains of the mice were removed after deep anesthesia was transcardially perfused using pentobarbital sodium 24 h after the SAH. Additionally, tissue from the right hemisphere was collected. In the cell culture experiments, cells were collected 24 h after hypoxia induction and thrombin treatment. Ten milliliters of ice-cold radioimmunoprecipitation assay lysis buffer and protease/

phosphatase inhibitor per gram of tissue were used for homogenization (Sigma–Aldrich Co.). After centrifugal separation (12,000×*g* for 30 min at 4 °C), the supernatants from the samples were collected. Ten μg of the protein (*in vivo*) and 0.8 μg of protein samples (*in vitro*) were applied onto the 5%–20% gradient sodium dodecyl sulfate polyacrylamide gels (SuperSep Ace; Wako Pure Chemicals; Osaka, Japan); electrophoresis was used to separate the solution according to molecular weight. The separated proteins were transferred to polyvinylidene fluoride membranes (Immobilon-P; Millipore Corporation; Billerica, MA, USA). The following primary antibodies were used: rabbit anti-thrombin (1:1000; Abcam; MA, USA), rabbit anti-prothrombin (1:1000; Abcam), rabbit anti-matrix metalloproteinase (MMP-9) (1:1000; Abcam), rabbit anti-phospho-p38 (1:1,000, Cell Signaling Technology, MA, USA), rabbit anti p38 (1:1,000, Cell Signaling Technology), rabbit anti-intercellular adhesion molecule (ICAM-1) (1:1,000, Cell Signaling Technology), and monoclonal anti-β-actin (1:2000; Sigma–Aldrich). The following secondary antibodies were used: anti-rabbit immunoglobulin G (IgG) (1:1000; Thermo Scientific; MA, USA) and anti-mouse IgG (1:1000; Pierce Biotechnology, Rockford, IL, USA). Immunoreactive bands were visualized using a Lumino imaging analyzer (LAS-4000; Fujifilm; Tokyo, Japan). Multi Gauge software (Fujifilm; Tokyo, Japan) was used to analyze the differences in band intensity.

2.9.1. Experiment 1

In this experiment, SAH was induced in 88 mice to evaluate the effect of nafamostat on early brain injury. Among them, 15 mice (17%) were excluded from the evaluation because of procedural failure (5 mice, 5.7%) or death (10 mice, 11.3%). The remaining 73 mice (8: Sham; 21: Vehicle; 13: nafamostat 0.1 mg/kg; and 21: nafamostat 1 mg/kg) were included for further investigation.

2.9.2. Experiment 2

SAH was induced in 16 male ddY mice to evaluate the relationship between SAH grading score and Hb assay. Among them, 2 mice were excluded from the evaluation due to death. Finally, 14 mice were assigned to the study, and the SAH grading score and Hb assay were evaluated.

2.9.3. Experiment 3

A total of ten male ddY mice (8 weeks, 5 control, and 5 nafamostat: 1 mg/kg) were induced in this experiment to evaluate the effect of nafamostat on coagulation time. Coagulation time was evaluated 1 h after the administration of 5% glucose (vehicle) or nafamostat (1 mg/kg).

2.10. Statistical analysis

CBF values are expressed as the mean ± the standard deviation, and western blotting and coagulation time are expressed as the mean ± the standard error. Counting and measurements were performed by blinded observers. Commercially available software (JMP 14; SAS Institute Inc., Cary, NC, USA) was used for all statistical analyses. Student's *t*-test or Welch's *t*-test (for parametric values) and Wilcoxon signed-rank test (for nonparametric values) were used for comparisons between the two experimental groups. One-way analysis of variance followed by Dunnett's test or Steel–Dwass tests for multiple pairwise comparisons. The Shapiro Wilk test was used to analyze data normality. Differences were considered statistically significant at $p < 0.05$.

3. Results

3.1. Nafamostat improved the neurological behavior after SAH

The time course of the experiment is shown in Fig. 1A. Nafamostat (5% glucose) was administered intraperitoneally at 0, 2, 4, and 6 h after SAH. CBF was measured in three periods (pre-procedure, post-procedure, and 1 d post-procedure), and neurological behavior tests were performed 1 d post-procedure. Representative images of CBF using the LSFI are shown in Fig. 1B. A significant decrease was observed in CBF (% con) from post to 1 d after the SAH in all groups (vs. pre, $p < 0.01$ in all groups, Fig. 1C). The total score of the neurological behavior test is shown in Fig. 1D. A significant improvement was observed in the neurological behavior of the nafamostat 1 mg/kg group compared with vehicle group (10.9 ± 5.87 vs. 14.3 ± 5.33, $p = 0.025$). The subscores of mNS in the vehicle and nafamostat 1 mg/kg group were shown in Fig. 1E. Significant differences were observed between four subscores (vibrissae touch; 1.36 ± 0.96 vs. 1.93 ± 0.86, $p = 0.039$, visual; 0.69 ± 0.99 vs. 1.29 ± 0.96, $p = 0.029$, forelimb use; 1.40 ± 0.72 vs. 1.81 ± 0.73, $p = 0.041$, hindlimb; 1.69 ± 0.62vs. 2.24 ± 0.52, $p = 0.004$, respectively). Based on these results, no CBF changes were observed after nafamostat administration post-SAH; neurological outcomes were improved.

3.2. Nafamostat administration after SAH did not increase the hemorrhagic volume

First, the relationship between SAH grading score and Hb assay was evaluated 1 d post-procedure. A representative picture of the SAH grading score is presented in Fig. 2A; additionally, a scatter plot regarding hemorrhage volume and SAH grading score is shown on Fig. 2B. A significant relationship was observed between the SAH grading score and the Hb assay. This indicates the potential of SAH grading score as an accurate evaluation method for SAH volume.

Second, the effect of nafamostat on SAH volume was evaluated. Digital images of the SAH and SAH grading scores for each group are shown in Fig. 2C and D. No significant differences were observed in the SAH grading score of each group. This indicates that nafamostat administration after SAH did not increase the hemorrhagic volume.

Finally, the effect of nafamostat on coagulation time was evaluated. Coagulation time was measured after the nafamostat administration. The APTT and PT results are shown in Fig. 2E. The prolongation in the APTT of the nafamostat administration group was observed; however, the difference was not significant.

3.3. Mechanisms underlying the protective effects of nafamostat

Western blotting was conducted to analyze right brain hemisphere tissues 24 h after SAH to investigate the mechanisms underlying the protective effects of nafamostat against the early brain injury (Fig. 3). Thrombin, active MMP-9, total MMP-9, and prothrombin were significantly upregulated at 24 h after the SAH induction which was suppressed by 1 mg/kg of nafamostat. The total MMP-9 protein was evaluated by assessing the total amount of active and pro MMP-9.

3.4. Effect of nafamostat on the in vitro combined thrombin and hypoxia model

The effects of nafamostat on *in vitro* combined thrombin and hypoxia stress using HBMVECs to further investigate the mechanisms

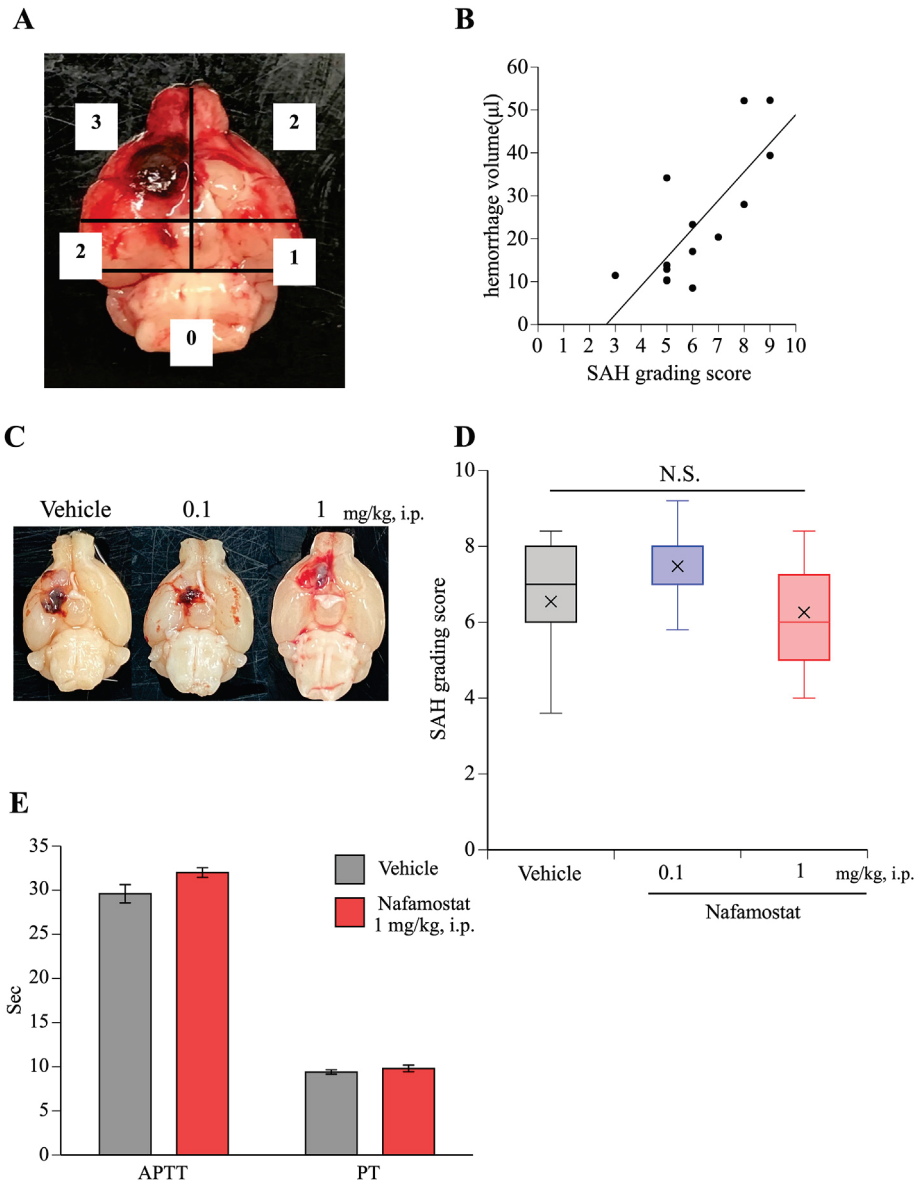

Fig. 2. The effect of nafamostat on hemorrhagic volume. (A) The representative picture of SAH grading score. (B) The hemorrhagic volume measured by using Hb assay correlated with SAH grading score, n = 14. Representative case of SAH grade (C) and quantitative data of SAH grade (D) on each group, Vehicle, n = 21; nafamostat 0.1 mg/kg, n = 13; nafamostat 1 mg/kg, n = 21, Steel–Dwass tests. (E) The coagulation time at 1 h after the nafamostat or 5% glucose administration, Vehicle, n = 5; nafamostat 1 mg/kg, n = 5. Nafamostat did not increase the hemorrhagic volume after the SAH.

underlying the protective effects of nafamostat. Thrombin was significantly upregulated and CBF was significantly decreased after SAH (*in vivo*); therefore, thrombin and hypoxia stress were induced to mimic the SAH state. The protocol used in this study is shown in Fig. 4A. Combination administration of thrombin and induction of hypoxia after 24 h promoted the phosphorylation of p38 and expression of ICMA-1 in HBMVECs. However, nafamostat treatment suppressed the phosphorylation of p38 from 0.1 to 10 μM (Fig. 4B), and the expression of ICAM-1 at 10 μM (Fig. 4C), after 24 h of thrombin and hypoxia treatment.

4. Discussion

This study primarily found the effectiveness of nafamostat in improving neurological outcomes through thrombin suppression and MMP-9 activation after SAH. Additionally, nafamostat exerted protective effects for HBMVECs from thrombin and hypoxia induction.

It has been reported that the up-regulation of microthrombi during the ultra-early phase of SAH which may aggravate delayed cerebral ischemia.[22–24] The increase in microthrombi after SAH is associated with an increase in thrombin, a protein that catalyzes the conversion of fibrinogen to fibrin.[25] In the present study, nafamostat inhibited the activation of thrombin after SAH which resulted in the suppression of microthrombi formation. Furthermore, thrombin is involved in brain edema and BBB disruption after cerebral ischemia and intracerebral hemorrhage.[13–15] It has been reported that argatroban exerts a protective effect against early brain injury after SAH due to its anti-thrombin activity.[16] In this report, argatroban improved neurological outcomes after acute SAH by suppressing BBB destruction, brain edema, and cell death, suggesting the effective of Xa inhibitor for SAH. In the present

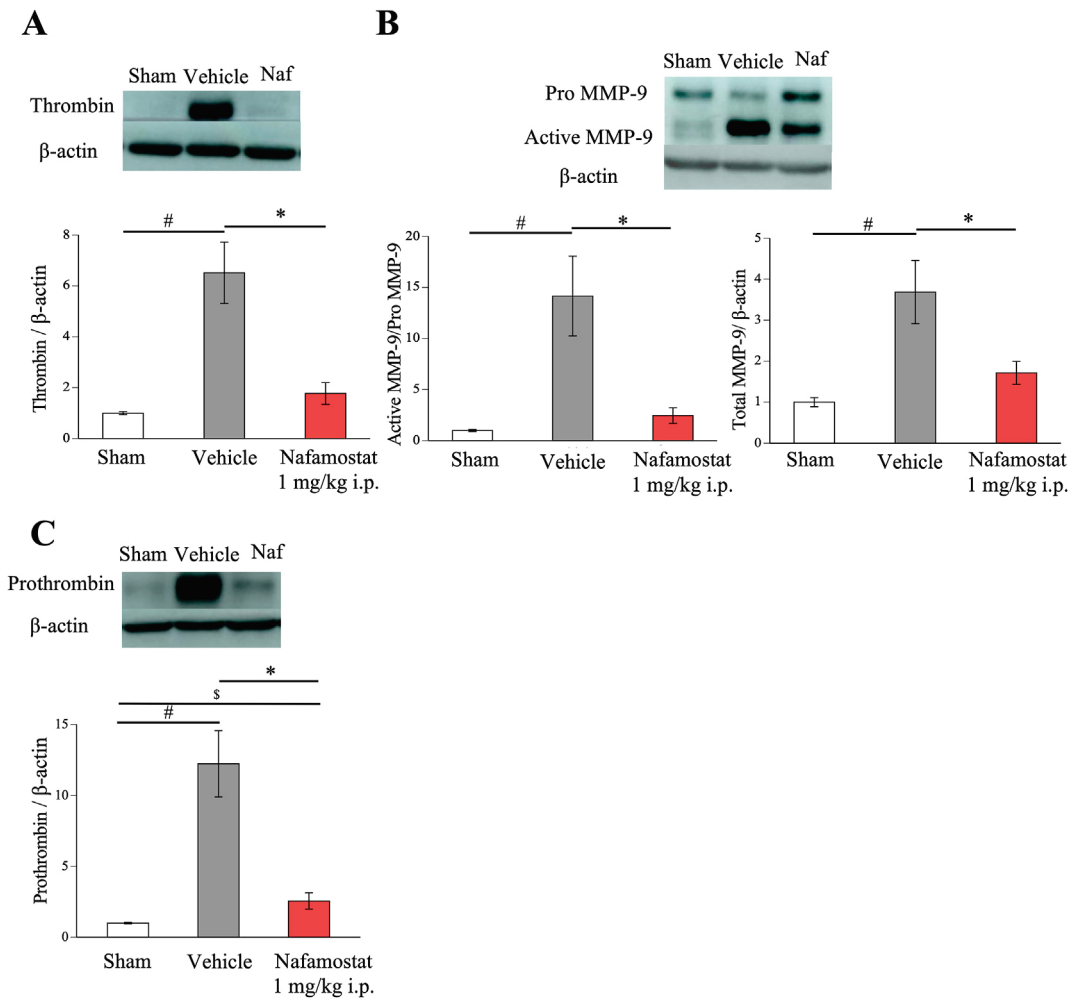

Fig. 3. The effect of nafamostat on thrombin, MMP-9, and prothrombin after the SAH. Western blotting was analyzed using right brain tissue at 24 h after the SAH. The effect of nafamostat on thrombin, MMP-9, are prothrombin are shown at (A) to (C). Data are expressed as means ± standard errors of the mean. n = 4 or 5 per group. $^{\#}p < 0.05$, sham vs. vehicle, $^{\$}$ $p < 0.05$, sham vs. 1 mg/kg, *$p < 0.05$, vehicle vs. 1 mg/kg, Wilcoxon signed-rank test.

study, nafamostat improved the neurological outcome after SAH (Fig. 1D). However, only four subscores of mNS were improved (Fig. 1E). Median values were improved even in subscore, indicating that nafamostat contributed to the improvement of neurological disability after SAH. In particular, protection of ischemic brain damage by inhibition of microthrombi may have been more likely to improve focal symptoms (paralysis or whisker sensation etc.).

In the present study, we also evaluated the prothrombin protein by western blotting. Prothrombin was up-regulated by SAH induction, and which was suppressed by nafamostat like thrombin. This result suggested that nafamostat inhibited the microthrombi by the suppression of prothrombin and thrombin.

MMP-9 is a well-known factor in brain edema after several brain injuries. Previous report showed that thrombin brain pericytes release high levels of MMP-9 in response to thrombin,[26] therefore, thrombin inhibition during early brain injury resulted in the suppression of MMP-9 expression. These effects may have resulted in improvements of the patient's neurological outcomes.

Previous reports have demonstrated the protective effect of nafamostat against vasospasm after the SAH.[11,12] However, this study found no effect of nafamostat on CBF during acute phase after the SAH. Intracranial changes immediately after the onset of SAH were more severe compared to the spasm phase. Nafamostat exhibits a vasodilator effect; however, this may be insufficient in contributing to the improvement of CBF. Additionally, this result may be due to the use of LSFI in measuring CBF only in the cerebral cortex; which may not be reflective of the blood flow of the whole brain. Therefore, further investigations will be needed to determine the effects of nafamostat on deep brain blood flow, particularly by using like two-photon microscopy.

In the present study, we evaluated the effects of nafamostat on *in vitro* combined thrombin and hypoxia stress using HBMVECs. There are several reports using hypoxia and thrombin to mimic the SAH,[27] and using thrombin + OGD model to mimic ischemic stroke.[10,21] In the present study, we adopted the hypoxia + thrombin model because the vivo experimental results showed that SAH increased thrombin expression in the brain and significantly decreased CBF.

Thrombin signaling in the endothelium is mediated by a protease-activated receptors (PARs). Four members of the PAR family have been identified, and PAR-1 is known as a thrombin receptor.[28] However, in the present study, we did not examine the expression of PAR-1, but we observed the changes in its downstream components, p38 and ICAM-1, suggesting that PAR-1 was the target of thrombin action. Previous reports indicated the PAR-1 activation on endothelial cell has been shown to increase the

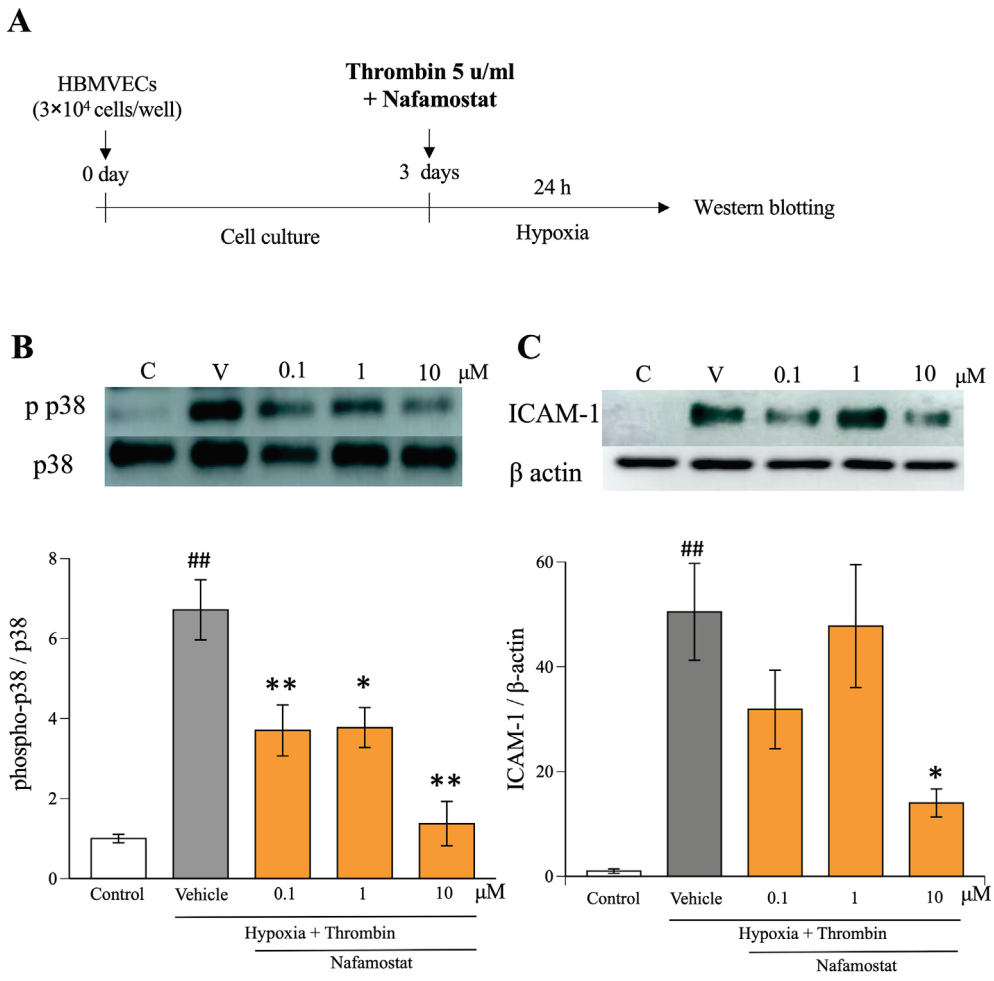

Fig. 4. The effect of nafamostat on human brain microvascular endothelial cells (HBMVECs) after thrombin and hypoxia stress. (A) The experimental protocol used to assess the effects of nafamostat against combined thrombin and hypoxia stress in HBMVECs. The effect of nafamostat on phosphorylation of p38 (B) and expression of ICAM-1 (C) 24 h after the thrombin and hypoxia stress. Data are expressed as means ± standard errors of the mean. n = 5 or 6 per group. $^{\#\#}p < 0.01$, sham vs. vehicle, Student's *t*-test. $^{*}p < 0.05$, $^{**}p < 0.01$, vs. vehicle, Dunnett's test.

expression of genes involved in cell proliferation, inflammation, leukocyte adhesion, vasomotion, and hemostasis.[29] Other reports have shown that after PAR-1 is activated in endothelial cells, the pathway regulates ICAM-1 expression via PI3K and Akt,[30] and via PKCδ-p38.[31] Based on the results of Fig. 4, nafamostat suppresses the phosphorylation of p38, leading to the suppression of ICAM-1.

Thrombin exerts a pro-inflammatory effect by increasing ICAM-1 expression in endothelial cells.[29] Additionally, experimental stroke models demonstrated that ICAM-1 is a key factor leading to BBB disruption, brain edema, and neuroinflammation.[32,33] In patients with severe COVID-19, elevated ICAM-1 expression has been reported.[34] Patients with severe disease are at an increased risk of developing inflammation and thrombosis; considering this, elevated ICAM-1 expression may be a factor that worsens prognosis. p38 is a protein involved in ICAM-1 regulation,[29] furthermore, it plays an important role in the cascade of inflammation and apoptosis, and is reportedly associated with worse prognosis after cerebral ischemic stroke and intracerebral hemorrhage.[35,36] In an SAH experimental model, Chen S et al. have reported that a p38 inhibitor suppressed the early brain injury.[37] In the present study, nafamostat suppressed the expression of p38 and ICAM-1, which resulted in endothelial protection during thrombin and hypoxia treatment. Nafamostat suppressed the expression of thrombin (Fig. 3), through suppression of p38 phosphorylation and ICAM-1 downstream of thrombin receptor, PAR-1. ICAM-1 is an important prognostic factor after stroke. Therefore, the suppression of thrombin after SAH by nafamostat may have contributed to the improvement of neurological findings by suppressing the expression of ICAM-1.

Taken together, the use of nafamostat in the early treatment of SAH may be a potential therapeutic approach contributing to a favorable outcome.

Nafamostat showed the endothelial protection from thrombin and hypoxia which improved neurological behavior after SAH. These findings indicate that early intervention after SAH using nafamostat reduces brain injury and improves neurological outcomes.

Declaration of competing interest

The authors declare that there are no COI.

Acknowledgments

None.

References

1. Geraghty JR, Testai FD. Delayed cerebral ischemia after subarachnoid hemorrhage: beyond vasospasm and towards a multifactorial pathophysiology. *Curr Atherosclerosis Rep*. 2017;19(12):50.
2. Egashira Y, Zhao H, Hua Y, Keep RF, Xi G. White matter injury after subarachnoid hemorrhage: role of blood-brain barrier disruption and matrix metalloproteinase-9. *Stroke*. 2015;46(10):2909–2915.
3. Fumoto T, Naraoka M, Katagai T, Li Y, Shimamura N, Ohkuma H. The role of oxidative stress in microvascular disturbances after experimental subarachnoid hemorrhage. *Transl Stroke Res*. 2019;10(6):684–694.
4. Fujii M, Yan J, Rolland WB, Soejima Y, Caner B, Zhang JH. Early brain injury, an evolving frontier in subarachnoid hemorrhage research. *Transl Stroke Res*. 2013;4(4):432–446.
5. Zhou P, Yang XL, Wang XG, et al. A pneumonia outbreak associated with a new coronavirus of probable bat origin. *Nature*. 2020;579(7798):270–273.
6. Yamamoto M, Kiso M, Sakai-Tagawa Y, et al. The anticoagulant nafamostat potently inhibits SARS-CoV-2 S protein-mediated fusion in a cell fusion assay system and viral infection in vitro in a cell-type-dependent manner. *Viruses*. 2020;12(6).
7. Yamamoto M, Matsuyama S, Li X, et al. Identification of nafamostat as a potent inhibitor of Middle East respiratory syndrome coronavirus S protein-mediated membrane fusion using the split-protein-based cell-cell fusion assay. *Antimicrob Agents Chemother*. 2016;60(11):6532–6539.
8. Chen T, Wang J, Li C, et al. Nafamostat mesilate attenuates neuronal damage in a rat model of transient focal cerebral ischemia through thrombin inhibition. *Sci Rep*. 2014;4:5531.
9. Liu Y, Li C, Wang J, et al. Nafamostat mesilate improves neurological outcome and axonal regeneration after stroke in rats. *Mol Neurobiol*. 2017;54(6):4217–4231.
10. Wang J, Li C, Chen T, et al. Nafamostat mesilate protects against acute cerebral ischemia via blood-brain barrier protection. *Neuropharmacology*. 2016;105:398–410.
11. Zhang Z, Nagata I, Kikuchi H, et al. Broad-spectrum and selective serine protease inhibitors prevent expression of platelet-derived growth factor-BB and cerebral vasospasm after subarachnoid hemorrhage: vasospasm caused by cisternal injection of recombinant platelet-derived growth factor-BB. *Stroke*. 2001;32(7):1665–1672.
12. Ghali MGZ, Srinivasan VM, Johnson J, Kan P, Britz G. Therapeutically targeting platelet-derived growth factor-mediated signaling underlying the pathogenesis of subarachnoid hemorrhage-related vasospasm. *J Stroke Cerebrovasc Dis*. 2018;27(9):2289–2295.
13. Kitaoka T, Hua Y, Xi G, Hoff JT, Keep RF. Delayed argatroban treatment reduces edema in a rat model of intracerebral hemorrhage. *Stroke*. 2002;33(12):3012–3018.
14. Nagatsuna T, Nomura S, Suehiro E, Fujisawa H, Koizumi H, Suzuki M. Systemic administration of argatroban reduces secondary brain damage in a rat model of intracerebral hemorrhage: histopathological assessment. *Cerebrovasc Dis*. 2005;19(3):192–200.
15. Ohyama H, Hosomi N, Takahashi T, Mizushige K, Kohno M. Thrombin inhibition attenuates neurodegeneration and cerebral edema formation following transient forebrain ischemia. *Brain Res*. 2001;902(2):264–271.
16. Sugawara T, Jadhav V, Ayer R, Chen W, Suzuki H, Zhang JH. Thrombin inhibition by argatroban ameliorates early brain injury and improves neurological outcomes after experimental subarachnoid hemorrhage in rats. *Stroke*. 2009;40(4):1530–1532.
17. Matsubara H, Imai T, Yamada T, et al. Importance of CBF measurement to exclude concomitant cerebral infarction in the murine endovascular perforation SAH model. *J Stroke Cerebrovasc Dis*. 2020;29(11):105243.
18. Matsumura K, Kumar TP, Guddanti T, Yan Y, Blackburn SL, McBride DW. Neurobehavioral deficits after subarachnoid hemorrhage in mice: sensitivity analysis and development of a new composite score. *J Am Heart Assoc*. 2019;8(8), e011699.
19. Sugawara T, Ayer R, Jadhav V, Zhang JH. A new grading system evaluating bleeding scale in filament perforation subarachnoid hemorrhage rat model. *J Neurosci Methods*. 2008;167(2):327–334.
20. Imai T, Iwata S, Miyo D, Nakamura S, Shimazawa M, Hara H. A novel free radical scavenger, NSP-116, ameliorated the brain injury in both ischemic and hemorrhagic stroke models. *J Pharmacol Sci*. 2019;141(3):119–126.
21. Li C, Wang J, Fang Y, et al. Nafamostat mesilate improves function recovery after stroke by inhibiting neuroinflammation in rats. *Brain Behav Immun*. 2016;56:230–245.
22. Clarke JV, Suggs JM, Diwan D, et al. Microvascular platelet aggregation and thrombosis after subarachnoid hemorrhage: a review and synthesis. *J Cerebr Blood Flow Metabol*. 2020;40(8):1565–1575.
23. Sabri M, Ai J, Lakovic K, Macdonald RL. Mechanisms of microthrombosis and microcirculatory constriction after experimental subarachnoid hemorrhage. *Acta Neurochir Suppl*. 2013;115:185–192.
24. Wang Z, Chen J, Toyota Y, Keep RF, Xi G, Hua Y. Ultra-early cerebral thrombosis formation after experimental subarachnoid hemorrhage detected on T2* magnetic resonance imaging. *Stroke*. 2021;52(3):1033–1042.
25. Pisapia JM, Xu X, Kelly J, et al. Microthrombosis after experimental subarachnoid hemorrhage: time course and effect of red blood cell-bound thrombin-activated pro-urokinase and clazosentan. *Exp Neurol*. 2012;233(1):357–363.
26. Machida T, Takata F, Matsumoto J, et al. Brain pericytes are the most thrombin-sensitive matrix metalloproteinase-9-releasing cell type constituting the blood-brain barrier in vitro. *Neurosci Lett*. 2015;599:109–114.
27. Nakagomi T, Kassell NF, Sasaki T, et al. Effect of hypoxia on endothelium-dependent relaxation of canine and rabbit basilar arteries. *Acta Neurochir*. 1989;97(1–2):77–82.
28. Vu TK, Hung DT, Wheaton VI, Coughlin SR. Molecular cloning of a functional thrombin receptor reveals a novel proteolytic mechanism of receptor activation. *Cell*. 1991;64(6):1057–1068.
29. Minami T, Sugiyama A, Wu SQ, Abid R, Kodama T, Aird WC. Thrombin and phenotypic modulation of the endothelium. *Arterioscler Thromb Vasc Biol*. 2004;24(1):41–53.
30. Rahman A, True AL, Anwar KN, Ye RD, Voyno-Yasenetskaya TA, Malik AB. Galpha(q) and Gbetagamma regulate PAR-1 signaling of thrombin-induced NF-kappaB activation and ICAM-1 transcription in endothelial cells. *Circ Res*. 2002;91(5):398–405.
31. Rahman A, Anwar KN, Uddin S, et al. Protein kinase C-delta regulates thrombin-induced ICAM-1 gene expression in endothelial cells via activation of p38 mitogen-activated protein kinase. *Mol Cell Biol*. 2001;21(16):5554–5565.
32. Li W, Suwanwela NC, Patumraj S. Curcumin prevents reperfusion injury following ischemic stroke in rats via inhibition of NF-κB, ICAM-1, MMP-9 and caspase-3 expression. *Mol Med Rep*. 2017;16(4):4710–4720.
33. Yang JT, Lee TH, Lee IN, Chung CY, Kuo CH, Weng HH. Dexamethasone inhibits ICAM-1 and MMP-9 expression and reduces brain edema in intracerebral hemorrhagic rats. *Acta Neurochir*. 2011;153(11):2197–2203.
34. Tong M, Jiang Y, Xia D, et al. Elevated expression of serum endothelial cell adhesion molecules in COVID-19 patients. *J Infect Dis*. 2020;222(6):894–898.
35. Ding Y, Flores J, Klebe D, et al. Annexin A1 attenuates neuroinflammation through FPR2/p38/COX-2 pathway after intracerebral hemorrhage in male mice. *J Neurosci Res*. 2020;98(1):168–178.
36. Uzdensky AB. Apoptosis regulation in the penumbra after ischemic stroke: expression of pro- and antiapoptotic proteins. *Apoptosis*. 2019;24(9–10):687–702.
37. Chen S, Ma Q, Krafft PR, et al. P2X7 receptor antagonism inhibits p38 mitogen-activated protein kinase activation and ameliorates neuronal apoptosis after subarachnoid hemorrhage in rats. *Crit Care Med*. 2013;41(12):e466–e474.